2	dispersal
3	
4	Davide Oppo ¹ , Christopher A-L Jackson ² , and Vittorio Maselli ³
5	¹ Sedimentary Basins Research Group, School of Geosciences, University of Louisiana at
6	Lafayette, Lafayette 70503, LA, US
7	² Landscapes and Basins Research Group (LBRG), Department of Earth Science &
8	Engineering, Imperial College, Prince Consort Road, London, SW7 2BP, UK
9	³ Università degli Studi di Modena e Reggio Emilia, Via Università 4, 41121, Modena, Italy.
10	
11	
12	
13	This manuscript is a preprint and is submitted for publication to a scientific journal. As a function of the peer-
14	reviewing process, its structure and content may change. If accepted, the final version of this manuscript will be
15	available via the 'Peer-reviewed Publication DOI' link on the right-hand side of this webpage. Please feel free to
16	contact any of the authors; we welcome feedback.
17	
18	
19	

Early extensional salt tectonics controls deep-water sediment

21

22

23

24

25

26

27

28

29

30

31

32

33

34

35

36

37

38

39

ABSTRACT

Predicting the distribution of sedimentary facies during the early stages of deformation of salt-detached continental margins is key to constraining the location and stratigraphic architecture of hydrocarbon and CO₂ reservoirs, as well as understanding the oceanic carbon cycle. Despite its importance, we still have a relatively poor understanding of salt-sediment interactions during the early phases of extensional salt tectonics, mainly because subsequent salt-related deformation and/or deep burial of the related stratigraphic succession means the related deposits are poorly imaged in seismic reflection data and/or not penetrated by borehole data. Using 3D seismic reflection data from the northern Levant Basin offshore Lebanon, here we investigate the interplay between early extension-related salt deformation and deep-water sediment dispersal. Our results indicate that salt tectonics has two contrasting impacts: whereas slope-parallel faults favor early sediment transfer along downslope-oriented corridors to the abyssal plain, slope-normal faults and ramp-syncline basins trap land-derived sediments hampering or delaying their transport to the abyssal plain. These results help refine source-to-sink models of turbidite systems developing in young salt basins and highlight the crucial role of extensional tectonics in the early stages of basin development, emphasizing the impact of fault strike, ramp-syncline basin evolution, and salt welding on deep-water sediment routing. Our study has significant implications for predicting deep-water stratigraphy in mature, more structurally complex basins.

40

41

42

43

44

INTRODUCTION

Determining how slope to deep-water sediment dispersal systems interact with seafloor structures is key to understanding how, how much, and where sediment is trapped along continental margins or, conversely, delivered to ocean basins. The distribution of sedimentary facies along continental margins can provide insights into how Earth's climatic and oceanographic system has changed over geological timescales, and the role played by deep-water depositional systems in sequestering carbon (Kennedy and Wagner, 2011; Mignard et al., 2017, 2017; McNeill et al., 2019; Graves et al., 2022; Liu et al., 2023). Predicting the distribution and stratigraphic architecture of sedimentary deep-water facies along continental margins can also guide resource exploration and utilization. For example, sandstone-dominated deep-water systems typically thin, onlap, and undergo complex lithological changes towards syn-depositional salt structures, thereby controlling the distribution, architecture, and ultimate performance of related hydrocarbon and carbon (i.e., Carbon Capture and Storage or 'CCS') reservoirs (Niemi et al., 2017; Gray et al., 2022). Salt tectonics has a profound impact on slope structure and the overall evolution of sediment deposition along continental margins, meaning salt basins are a key archive for recording past geological change through their stratigraphic record (Pichel et al., 2018; Oppo et al., 2023). For example, numerous studies have focused on how salt-induced deformation and sediment gravity currents, such as turbidity currents and debris flows, interact with seabed structures to build deep-water channels and lobes (e.g., Loncke et al., 2006; Gee and Gawthorpe, 2006; Oluboyo et al., 2014; Howlett et al., 2021). These studies have typically focused on the distal, contraction-dominated parts of mature salt-tectonic systems (e.g., circum-Gulf of Mexico, offshore eastern Canada, circum-South Atlantic), where seafloor relief may trap or deflect sediment delivered from the basin margin, commonly resulting in fill-and-spill style depositional patterns (Galloway, 1975). In contrast, the impact of seafloor deformation in the updip, extension-dominated zone has been, to our knowledge, very rarely documented. The only notable exception is the study by Anderson et al. (2000), who show that long-term (c. 12 Myr) changes in fault-sediment interactions offshore Angola reflect gross variations in (salt-detached) fault-driven accommodation vs. sediment accumulation

45

46

47

48

49

50

51

52

53

54

55

56

57

58

59

60

61

62

63

64

65

66

67

68

69

rate. These variations are expressed as an overall decrease in confinement, principally driven by an increase in sediment supply.

Whereas interactions between salt-induced seafloor deformation and deep-water depositional systems are relatively well-characterized in modern (i.e., at- or near-seabed) systems developed in the distal parts of salt-influenced continental margins, they are poorly constrained during the early phases of deformation and basin development. This at least partly reflects the fact that subsequent salt-tectonic deformation and, in particular, subsidence leads to the deep burial (and thus poor seismic imaging) of the related stratigraphic record. Such interactions, in addition to ramp-syncline basins (RSB), a relatively common type of salt-related depocentre that forms slightly downdip of the extensional zone (e.g., Pichel et al., 2018), are not captured in generic models illustrating salt-sediment interactions on salt-detached slopes (e.g., Oluboyo et al., 2014; Cumberpatch et al., 2021; Howlett et al., 2021). For example, beyond containing landward-dipping and -thickening wedges of slope strata (e.g., Pichel et al., 2018), there has been no detailed documentation of the types of depositional systems deposited and preserved within RSBs.

Salt in the Mediterranean Sea is relatively young (<6 Myr) and as a result, it and its relatively seismically well-imaged overburden have yet to experience intense deformation. We therefore use 3D seismic reflection data from the northern Levant Basin, eastern Mediterranean, to investigate the relationship between early extension-related, salt-tectonic deformation and deep-water sediment dispersal, thereby helping refine source-to-sink models of salt-controlled depositional systems. Our results can be applied when trying to predict deep-water stratigraphy in more strongly deformed and/or deeply buried salt basins globally, where borehole data may be sparse and/or seismic reflection imaging poor.

GEOLOGICAL SETTING

The Miocene to recent stratigraphy of the Levant Basin comprises evaporites (Messinian Salt) capped by up to 2 km of predominantly deep-water clastic deposits (Haq et al., 2020; Kabir et al., 2022; Oppo et al., 2023). Messinian Salt and its overburden were moderately deformed in response to westward gravity gliding induced by post-Pleistocene tilting and uplift of the northern Levantine margin (Cartwright and Jackson, 2008). Salt-detached gliding produced kinematically linked zones of updip extension and downslope contraction. Our study area is located in the updip extensional zone, which is dominated by reactive diapirism associated with predominantly N-S-striking, basinward-dipping, and salt-detached normal faults, some of which are expressed on the present seafloor. Margin-normal (i.e., E-trending) reactive diapirs and associated salt-detached faults are also observed, in addition to ramp-syncline basins (Fig. 1) (Evans et al., 2021).

The post-Messinian deep-water stratigraphy in the North Levant Basin has, to the best of our knowledge, only been described by Maselli et al. (2021), who investigated the spatial and temporal evolution of bedforms in a single, near-seabed (i.e., Recent) deep-water lobe cut by a salt-detached normal fault. They highlighted that extensional salt tectonics has had and likely continues to play a key role in controlling deep-water sedimentation and stratigraphic development.

DATA AND METHODS

We use 3D time-migrated seismic reflection data that is near-zero phase at the seafloor reflection and is displayed here with SEG negative polarity, i.e., downward increase and decrease in acoustic impedance are represented by a trough (blue in our seismic displays) and peak (red in our seismic displays) reflection, respectively (Brown, 2001). The dominant frequency in the post-salt overburden, extracted directly from the seismic dataset, is 50 Hz, with an average P-wave velocity of 2,000 m/s indicated by proprietary processing reports.

Based on these data, the estimated vertical resolution for the post-salt overburden is ~10 m. The horizontal resolution is ~25 m, approximated as a quarter of the dominant wavelength (Lebedeva-Ivanova et al., 2018). As shown below, these data are of sufficient quality to image the main salt-tectonic structures and the key depositional elements in the overburden.

The lack of well data offshore Lebanon prevents a precise calibration of the lithology and age of the overburden. We therefore use seismic facies analysis and the amplitude root mean square (RMS) to infer depositional system types and sediment grain size. More specifically, following Maselli et al. (2021) and other studies of deep-water seismic geomorphology (e.g., Prather et al., 1998), we interpret high RMS values as representing coarser, likely sand-rich sediment. The only absolute age is provided by the 1.8 Ma reflection, correlated from Oppo et al. (2021). However, the excellent seismic data quality means we can confidently establish a robust seismic-stratigraphic framework to define the relative if not absolute age of various depositional elements.

RESULTS

In the south of the study area, a U-shaped incision extends from the shelf to the slope and is filled with generally high-amplitude, relatively continuous reflections. This incision is interpreted as a turbidite channel delivering sediments to the abyssal plain (Channel A) (Figs. 1, 2). Channel A extends from the base-of-slope to the abyssal plain, crossing the extensional zone, where it is confined laterally by margin-normal and -oblique faults that displace seismic reflections up to the seafloor (Figs.1, 3). In the easternmost, most proximal part of the survey, Channel A is underlain by stacked paleochannels that progressively migrate laterally. The oldest paleochannels developed at ca. 1.8 Ma, indicating this is a relatively long-lived system (Fig. 2A). Less than 5 km basinward, the stacked paleochannels disappear from the stratigraphy, and only the seabed expression of Channel A is present (Fig. 2B). Stacked

paleochannels are also absent throughout the extensional zone, where the channel stratigraphy is mainly formed by high-amplitude, variable continuity seismic reflections, which are locally preserved within margin-normal grabens (Figs. 3A, B).

Upon reaching the abyssal plain, Channel A encounters an RSB that contains sheet-like, high-amplitude reflections at its base, which we interpret as stacked deep-sea lobes, and which are variably incised by U-shaped stacked channels filled with high-amplitude reflections (Fig. 3C). Notably, in this location, the main channel, Channel A, is defined by relatively low-amplitude reflections, suggesting it is finer-grained than its encasing lobes (Figs. 3C, 4). Further basinward, the channel encounters a second RSB (Fig. 3D), where at least two stacked lobes, larger than the one in the updip RSB, occur. Like those in the updip RSB, these lobes are defined by high-amplitude reflections and are incised by a low-amplitude Channel A. Above the lobes, stacked channels transition to laterally continuous, high-amplitude reflections without clear channel incisions, which are visible only in the near-seafloor interval. We interpret these continuous reflections as a shallower, more recent lobe.

Once it exits the second RSB, the channel becomes less confined, with the underlying stratigraphy being defined by well-developed, reflective, presumably sandy paleochannels (Fig. 4). The stratigraphic relationship between the 1.8 Ma reflection and lobes in the downdip RSB/abyssal plain suggests that the onset of sandy deposition was broadly coincident with the initiation of the oldest paleo-channel observed in the most proximal part of the survey (Fig. 2A).

A second channel (Channel B) is present c. 8.6 km north of Channel A. Channel B shares many similarities with Channel A, i.e., it extends from the base-of-slope to the abyssal plain, crossing the salt-detached extensional zone (Fig. 1), and proximal to the base-of-slope is underlain by stacked paleochannels that developed after ca. 1.8 Ma (Fig. 2A), but which are absent from the stratigraphy immediately basinward of the first margin-parallel, salt-

related graben (Fig. 2B). Unlike Channel A, however, Channel B is not laterally confined by faults at the base-of-slope, where it instead trends slope-parallel. Further downslope, in the central, more heavily faulted area, the channel abruptly turns 90° northward upon entering a margin-parallel graben, and then 90° westward, where it exits the graben before passing onto the abyssal plain and becoming relatively sinuous (Fig. 1). Seismic sections across this tract of the channel show that it has an erosional base and is underfilled (Fig. 5A). On the abyssal plain, downslope of the extensional zone, Channel B has a moderately erosional base and is bounded by small levees (Fig. 5C), before passing downslope into at-seabed (i.e., Recent) lobes (Figs. 1C, 5B).

INTERPRETATION

Our data suggest that early salt deformation in the extensional zone of a salt-detached slope controlled the sequestration and routing of deep-water sediment and the ultimate stratigraphic evolution of related channels and lobes. We interpret two main styles of salt-sediment interaction: (1) early and sustained delivery of coarse-grained sediment to the abyssal plain (as exemplified by Channel A), and (2) initial sequestration of sediment at the base-of-slope, with subsequent bypass of the extensional zone (as exemplified by Channel B).

Channel A – Early delivery to the abyssal plain

The stratigraphic relationship between the paleochannels, the downslope paleo-lobes, and the 1.8 Ma reflection indicates that coarse-grained sediment supply to the abyssal plain was established in the Early Pleistocene. Time-equivalent paleochannels at the base-of-slope and on the abyssal plain indicate that Channel A connected these two areas despite the lack of obvious paleochannel-related incisions across the extensional zone. We interpret that the apparent absence of incision reflects the combined effects of structural confinement by

margin-normal and -oblique faults and related grabens, and the elevated sediment supply, which together caused channel filling, inhibited erosion, and aided basinward propagation of the channel. As a result, large volumes of coarse sediment were delivered through the extension zone directly to lobes on the abyssal plain.

195

196

197

198

199

200

201

202

203

204

205

206

207

208

209

210

211

212

213

214

215

216

217

218

219

Notably, however, upon reaching the abyssal plain, the salt-detached translation still influenced sedimentation patterns, with RSBs temporarily providing accommodation for the local preservation of lobes. More specifically, we infer that the deposition of a sandy lobe in the updip RSB was followed by channel incision and coarse sediment bypass to the downdip RSB, where a stacked set of sandy lobes were deposited before the channel was filled by finer-grained material. These lobes were then incised by their feeder channel, which propagated basinward, delivering sediments to the most distal part of the abyssal plain. We suggest that the shallowest lobe within the downdip RSB (Fig. 3D) formed during a period of reduced incision, possibly due to a reduced gradient and/or supply during higher sea level. The deposition of coarse-grained sediment within the RSB, and its subsequent incision by a younger channel that was ultimately filled by finer-grained material, records the progressive basinward migration of the slope depocenter and bypassing coarse sediment to the distal abyssal plain. These depositional patterns are comparable to those captured in deep-water filland-spill models, where the relationship between accommodation and sediment accumulation rates controls depocenter filling vs. bypass. In this example, salt-detached translation, rather than minibasin subsidence (e.g., Prather et al., 1998) or contractional growth folding (e.g., Smith, 2004), caused the local development of intra-slope accommodation. The rate of saltdetached translation and, by extension, accommodation development within an RSB are predominantly controlled by pulses of salt flow due to volumetric flux imbalances across underlying anticlines (Evans et al., 2021). Such pulses lead to cyclical variations in local translation rates, impacting how, where, and how much sediment is deposited or bypassed in

these highly dynamic systems. In particular, faster or slower translation rates result in the increase or decrease of accommodation, respectively. In the latter case, when the sediment supply is relatively high, the overall aggradation will also be high, giving rise to a fill-and-spill system. Given that thick, stacked lobe-dominated successions are not preserved in the documented RSBs, and that an overall fill-and-spill pattern is recorded, we suggest that RSB (horizontal) translation and (vertical) subsidence rate were low relative to sediment supply, thus favoring the delivery of coarse sediment to the distal basin in a relatively short period after channel establishment on the upper slope.

Channel B – Early sequestration at the base-of-slope

Based on their stratigraphic relationship to the 1.8 Ma reflection, we infer the paleochannels associated with Channel B also initiated in the Early Pleistocene, at broadly the same time as Channel A. However, the lack of paleochannels, paleo-lobes, and other stratigraphic evidence of coarse-grained sediment delivery to, or at least preservation within, the extension zone and abyssal plain indicates that Channel B did not reach the deeper basin until relatively recently. This indicates that the most proximal margin-parallel, intra-slope graben efficiently trapped coarse-grained sediment, stopping it from reaching the base-of-slope and abyssal plain. Like Channel A, the depositional patterns described here are comparable to those captured in deep-water fill-and-spill models. Critically, however, at least during the earliest phase of development of Channel B, we only observe the 'fill' phase.

Over time, Channel B migrated southwards, beyond the southern limit of the graben (Fig. 2A). This, possibly coupled with slower subsidence and accommodation development rate due to progressive salt welding, allowed the channel to ultimately escape from the graben and extend basinward. However, the channel was eventually (and continues to be) partly confined by the next downslope graben. Within this new depocentre, the strongly erosional

character of the channel (Fig. 5A) suggests that confinement favored (and perhaps still favors) sediment bypass through the entire upper course of the channel.

247

248

249

250

251

252

253

254

255

256

257

258

259

260

261

262

263

264

265

266

267

268

269

245

246

CONCLUSION AND IMPLICATIONS

Our study shows that extensional tectonics during the early stages of salt-detached extension profoundly controls sediment routing to the abyssal plain. More specifically, slopeparallel faults focus turbidity currents, favoring early sediment transfer through the extensional zone to the abyssal plain, whereas slope-normal faults and RSBs generate considerable accommodation, thus favoring trapping and deflection of deep-water channels and the accumulation of coarse sediment at the base-of-slope. In the latter case, those structures reduce the seafloor gradient and cause turbidity currents to decelerate, depositing the coarse-grained fractions and allowing the development of a lobe (Maselli et al., 2021). Possibly, the finer fractions continue distally and are presented by the low-amplitude sediment waves observed in the abyssal plain (Figs. 1A, C). Eventually, lateral channel migration and/or the cessation of accommodation generation due to salt welding allow the channel to transfer sediment toward and onto the abyssal plain. Therefore, the interplay between 1) the rate of the seaward flow of salt, 2) RSB translation rate and accommodation development, and 3) sediment supply and accumulation in RSBs dictates the evolution of coarse-grained sediment depocenters and, ultimately, delivery of material to ocean basins. Our study provides insights into likely salt-sediment interactions in other salt basins, such as those offshore Nova Scotia (e.g., Saint-Ange et al., 2017), Morocco (e.g., Uranga et al., 2022), and Brazil (e.g., Pichel et al., 2018), where the influence of RSB development on the stratigraphic evolution of deep-water systems has yet to be thoroughly investigated. The role of slope-parallel grabens and RSBs in trapping sediment within proximal,

base-of-slope areas could have significant implications for the complex dynamics of organic

carbon transport to the abyssal plain. Large volumes of carbon originating from land or shelf regions are transferred to the deep sea via turbidity currents (Galy et al., 2007; Pope et al., 2022; Talling et al., 2024), and may be temporarily or permanently stored in these grabens and within intra-RSB lobes, facilitated by high subsidence and sedimentation rates that rapidly isolate the carbon from the oxidizing conditions near the seafloor. Over time, variations in channel erosion rates could lead to the incision of the intra-RSBs lobes, resulting in the re-suspension and oxidation of previously buried carbon, which is reintroduced into the environment.

Our study highlights that fault strike relative to sediment input direction, RSB development and evolution, and the temporal relationship between sediment input and salt welding all need to be captured in tectonostratigraphic models for salt basins, given these dictate if and where land-derived material is delivered to the deep ocean. Our results also provide insights into early-stage, deep-water stratigraphic patterns in salt basins that are now strongly deformed in response to ongoing tectonics, thus helping reconstruct the distribution of sedimentary facies relevant for resource exploration and the oceanic carbon cycle in salt basins.

ACKNOWLEDGMENTS

We acknowledge W. Chbat and the Lebanese Petroleum Administration for providing data and Schlumberger for granting Petrel© academic licenses.

REFERENCES CITED

Anderson, J.E., Cartwright, J., Drysdall, S.J., and Vivian, N., 2000, Controls on turbidite sand deposition during gravity-driven extension of a passive margin: examples from Miocene sediments in Block 4, Angola: Marine and Petroleum Geology, v. 17, p. 1165–1203, doi:10.1016/S0264-8172(00)00059-3.

296 297	Brown, A.R., 2001, Color in seismic display: The Leading Edge, v. 20, p. 549–549, doi:10.1190/1.1438992.
298 299 300 301	Cartwright, J.A., and Jackson, M.P.A., 2008, Initiation of gravitational collapse of an evaporite basin margin: The Messinian saline giant, Levant Basin, eastern Mediterranean: Geological Society of America Bulletin, v. 120, p. 399–413, doi:10.1130/B26081X.1.
302 303 304 305	Cumberpatch, Z.A., Kane, I.A., Soutter, E.L., Hodgson, D.M., Jackson, C.AL., Kilhams, B.A., and Poprawski, Y., 2021, Interactions between deep-water gravity flows and active salt tectonics: Journal of Sedimentary Research, v. 91, p. 34–65, doi:10.2110/jsr.2020.047.
306 307 308	Evans, S.L., Jackson, C.AL., and Oppo, D., 2021, Taking the Pulse of Salt-Detached Gravity Gliding in the Eastern Mediterranean: Tectonics, v. 40, p. e2020TC006476, doi:https://doi.org/10.1029/2020TC006476.
309 310	Galloway, W.E., 1975, Process Framework for Describing the Morphologic and Stratigraphic Evolution of Deltaic Depositional Systems: Deltas: Models for Exploration, p. 87–98.
311 312 313	Galy, V., France-Lanord, C., Beyssac, O., Faure, P., Kudrass, H., and Palhol, F., 2007, Efficient organic carbon burial in the Bengal fan sustained by the Himalayan erosional system: Nature, v. 450, p. 407–410, doi:10.1038/nature06273.
314 315 316	Gee, M.J.R., and Gawthorpe, R.L., 2006, Submarine channels controlled by salt tectonics: Examples from 3D seismic data offshore Angola: Marine and Petroleum Geology, v. 23, p. 443–458, doi:10.1016/j.marpetgeo.2006.01.002.
317 318 319	Graves, C.A. et al., 2022, Sedimentary carbon on the continental shelf: Emerging capabilities and research priorities for Blue Carbon: Frontiers in Marine Science, v. 9, doi:10.3389/fmars.2022.926215.
320 321 322 323	Gray, E., Hartley, A., and Howell, J., 2022, The influence of stratigraphy and facies distribution on reservoir quality and production performance in the Triassic Skagerrak Formation of the UK and Norwegian Central North Sea: Geological Society, London, Special Publications, v. 494, p. 379–409, doi:10.1144/SP494-2019-68.
324 325 326	Haq, B., Gorini, C., Baur, J., Moneron, J., and Rubino, JL., 2020, Deep Mediterranean's Messinian evaporite giant: How much salt? Global and Planetary Change, v. 184, p. 103052, doi:10.1016/j.gloplacha.2019.103052.
327 328 329 330	Howlett, D.M., Gawthorpe, R.L., Ge, Z., Rotevatn, A., and Jackson, C.AL., 2021, Turbidites, topography and tectonics: Evolution of submarine channel-lobe systems in the salt-influenced Kwanza Basin, offshore Angola: Basin Research, v. 33, p. 1076–1110, doi:10.1111/bre.12506.
331 332 333 334 335	Kabir, S.M.M., Iacopini, D., Hartley, A., Maselli, V., and Oppo, D., 2022, Seismic characterization and depositional significance of the Nahr Menashe deposits: Implications for the terminal phases of the Messinian salinity crisis in the north-east Levant Basin, offshore Lebanon: Basin Research, v. 00, p. 1–26, doi:10.1111/bre.12697.

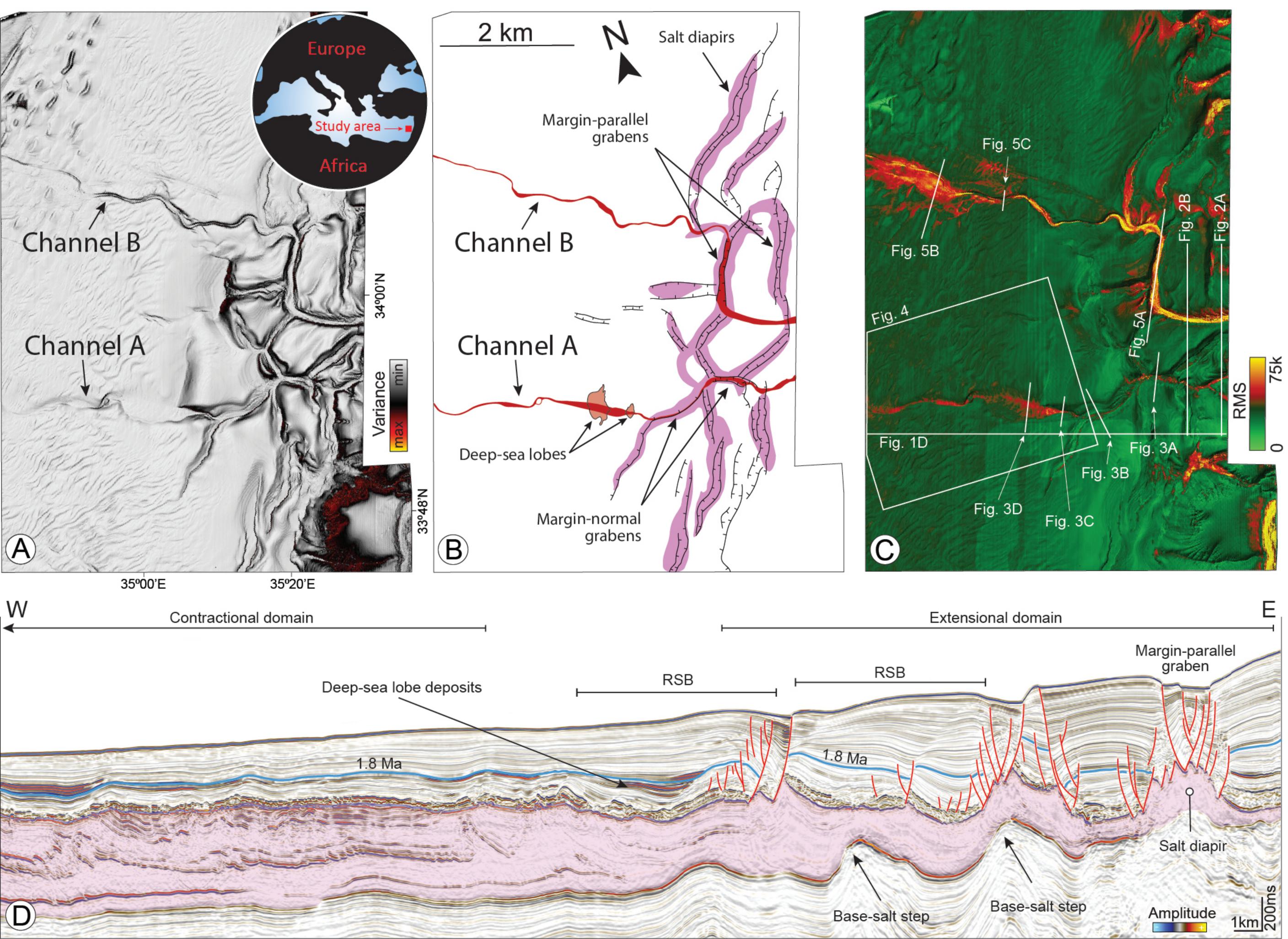
- Kennedy, M.J., and Wagner, T., 2011, Clay mineral continental amplifier for marine carbon
- sequestration in a greenhouse ocean: Proceedings of the National Academy of
- 338 Sciences, v. 108, p. 9776–9781, doi:10.1073/pnas.1018670108.
- Lebedeva-Ivanova, N., Polteau, S., Bellwald, B., Planke, S., Berndt, C., and Henriksen
- Stokke, H., 2018, Toward one-meter resolution in 3D seismic: The Leading Edge, v.
- 37, p. 794–864, doi:https://doi.org/10.1190/tle37110818.1.
- Liu, X., Fan, D., Xu, F., and Liu, J.P., 2023, Editorial: Sedimentation on the continental
- margins: From modern processes to deep-time records: Frontiers in Earth Science, v.
- 344 10, doi:10.3389/feart.2022.1048801.
- Loncke, L., Gaullier, V., Mascle, J., Vendeville, B., and Camera, L., 2006, The Nile deep-sea
- fan: An example of interacting sedimentation, salt tectonics, and inherited subsalt
- paleotopographic features: Marine and Petroleum Geology, v. 23, p. 297–315,
- 348 doi:10.1016/j.marpetgeo.2006.01.001.
- Maselli, V., Micallef, A., Normandeau, A., Oppo, D., Iacopini, D., Green, A., and Ge, Z.,
- 350 2021, Active faulting controls bedform development on a deep-water fan: Geology, v.
- 49, p. 1495–1500, doi:10.1130/G49206.1.
- McNeill, L.C. et al., 2019, High-resolution record reveals climate-driven environmental and
- sedimentary changes in an active rift: Scientific Reports, v. 9, p. 3116,
- doi:10.1038/s41598-019-40022-w.
- 355 Mignard, S.L.-A., Mulder, T., Martinez, P., Charlier, K., Rossignol, L., and Garlan, T., 2017,
- Deep-sea terrigenous organic carbon transfer and accumulation: Impact of sea-level
- variations and sedimentation processes off the Ogooue River (Gabon): Marine and
- 358 Petroleum Geology, v. 85, p. 35–53, doi:10.1016/j.marpetgeo.2017.04.009.
- Niemi, A., Bear, J., and Bensabat, J. (Eds.), 2017, Geological Storage of CO2 in Deep Saline
- Formations: Springer Dordrecht, 554 p., https://link.springer.com/book/10.1007/978-
- 361 94-024-0996-3 (accessed April 2024).
- Oluboyo, A.P., Gawthorpe, R.L., Bakke, K., and Hadler-Jacobsen, F., 2014, Salt tectonic
- controls on deep-water turbidite depositional systems: Miocene, southwestern Lower
- Congo Basin, offshore Angola: Basin Research, v. 26, p. 597–620,
- 365 doi:10.1111/bre.12051.
- Oppo, D., Evans, S., Iacopini, D., Kabir, S.M., Maselli, V., and Jackson, C.A.-L., 2021,
- Leaky salt: pipe trails record the history of cross-evaporite fluid escape in the northern
- Levant Basin, Eastern Mediterranean: Basin Research, v. 33, p. 1798–1819,
- 369 doi:https://doi.org/10.1111/bre.12536.
- Oppo, D., Jackson, C.A.-L., Gorini, C., Iacopini, D., Evans, S., and Maselli, V., 2023, Mass
- wasting records the first stages of the Messinian Salinity Crisis in the eastern
- 372 Mediterranean: Geology, v. 51, p. 637–641, doi:10.1130/G51146.1.
- Pichel, L.M., Peel, F., Jackson, C.A.-L., and Huuse, M., 2018, Geometry and kinematics of
- salt-detached ramp syncline basins: Journal of Structural Geology, v. 115, p. 208–230,
- 375 doi:10.1016/j.jsg.2018.07.016.

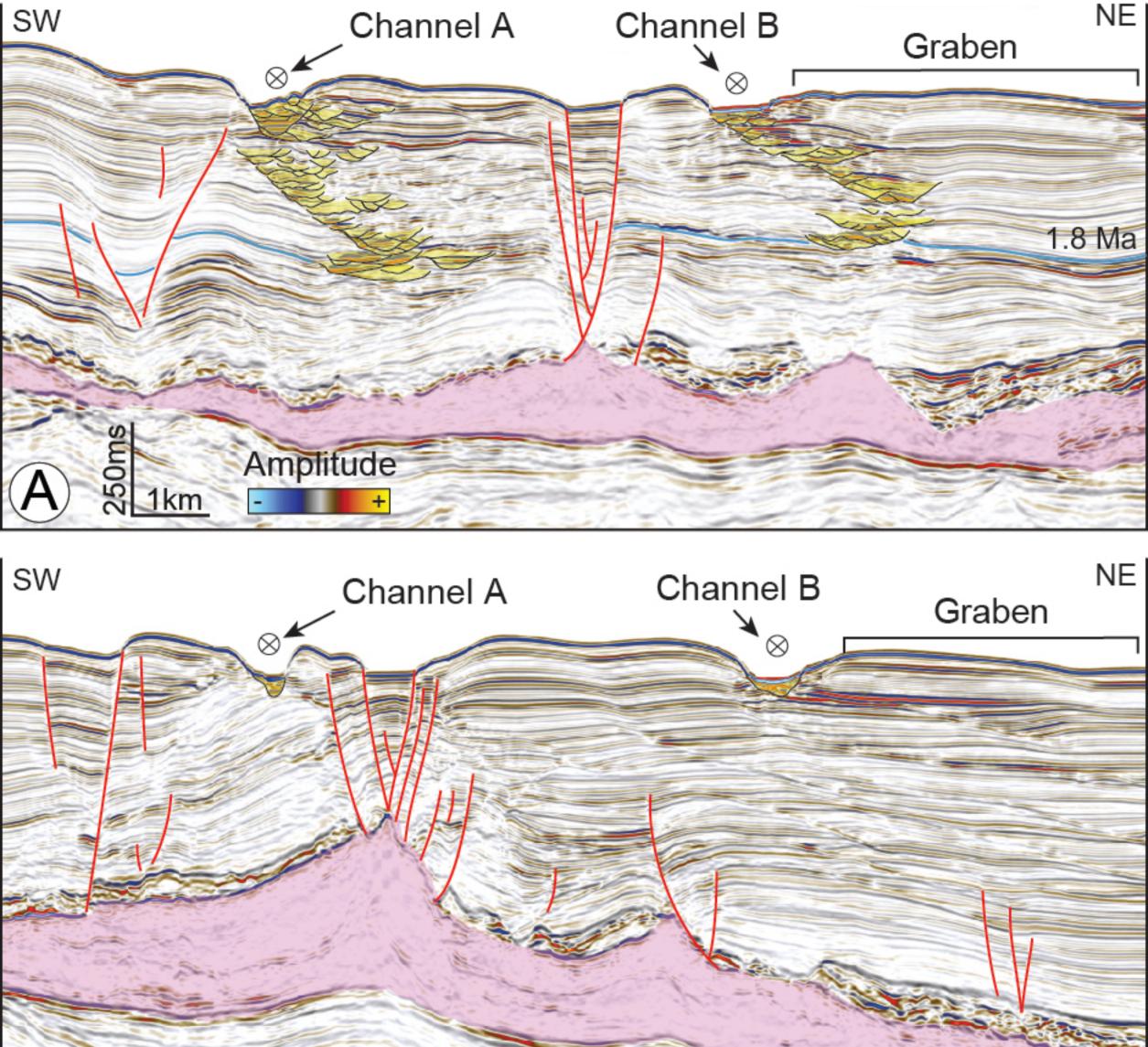
376 377 378	Pope, E.L. et al., 2022, Carbon and sediment fluxes inhibited in the submarine Congo Canyon by landslide-damming: Nature Geoscience, v. 15, p. 845–853, doi:10.1038/s41561-022-01017-x.
379 380 381 382	Prather, B.E., Booth, J.R., Steffens, G.S., and Craig, P.A., 1998, Classification, Lithologic Calibration, and Stratigraphic Succession of Seismic Facies of Intraslope Basins, Deep-Water Gulf of Mexico1: AAPG Bulletin, v. 82, p. 701–728, doi:10.1306/1D9BC5D9-172D-11D7-8645000102C1865D.
383 384	Saint-Ange, F., Savva, D., Colletta, B., Marfisi, E., Cuilhé, L., MacDonald, A., and Luheshi, M., 2017, Salt – sediment interaction in Sable Sub-basin, Nova Scotia (Canada).
385 386 387 388	Smith, R., 2004, Silled sub-basins to connected tortuous corridors: sediment distribution systems on topographically complex sub-aqueous slopes, <i>in</i> Lomas, S.A. and Joseph, P. eds., Confined Turbidite Systems, Geological Society of London, v. 222, p. 0, doi:10.1144/GSL.SP.2004.222.01.03.
389 390 391 392	Talling, P.J., Hage, S., Baker, M.L., Bianchi, T.S., Hilton, R.G., and Maier, K.L., 2024, The Global Turbidity Current Pump and Its Implications for Organic Carbon Cycling: Annual Review of Marine Science, v. 16, p. 105–133, doi:10.1146/annurev-marine-032223-103626.
393 394 395	Uranga, R.M., Ferrer, O., Zamora, G., Muñoz, J.A., and Rowan, M.G., 2022, Salt tectonics of the offshore Tarfaya Basin, Moroccan Atlantic margin: Marine and Petroleum Geology, v. 138, p. 105521, doi:10.1016/j.marpetgeo.2021.105521.
396	
397	
398	FIGURE CAPTIONS
399	Figure 1. (A) and (C) show the bathymetry of the study area using the variance and amplitude
400	RMS seismic attributes, respectively. (B) Structural map showing the two channels (red),
401	normal faults (black), and salt diapirs (pink). (C) The red/yellow color represents higher
402	concentrations of coarse-grained sediment. (D) Seismic section shows the overall margin
403	setting. Red faults are late to post-Messinian and are related to salt gliding toward the basin.
404	Pink shading: Messinian Salt. RSB: Ramp syncline basin. RMS: Root Mean Square.
405	
406	Figure 2. Seismic cross-sections parallel to the margin (location in Fig. 1C) showing the
407	channels evolution close to the base-of-slope. (A) Proximal seismic cross-section showing
408	stacked channels underneath both Channel A and Channel B. Note the progressive lateral

409 migration to the southwest. (B) Parallel seismic cross-section basinward to the first margin-410 parallel graben showing the absence of stacked paleochannels and only a relatively recent, 411 modern channel incising the seafloor. Faults are red, Messinian Salt is pink, and sand-rich 412 channels and lobes deposit in yellow. 413 414 Figure 3. Seismic cross-sections showing the lack of a well-developed Channel A incision within grabens (A) and half-grabens (B) across the extensional zone. (C-D) Well-developed 415 416 paleochannels and deep-sea lobes are associated with Channel A within the first (C) and the 417 second (D) RSB (Fig. 3 for location). Faults are red, Messinian Salt is pink, and sand-rich 418 channels and lobes deposit in yellow. 419 420 Figure 4. RMS amplitude calculated on the 1.8 Ma horizon showing the two deep-sea lobes 421 mainly formed by the deposition of coarse-grained sediment within two consecutive RSBs. 422 Note the low amplitude of Channel A when incising the distal lobe. The dashed lines delimit 423 the RSB. 424 425 Figure 5. Seismic cross-sections showing the basinward development of Channel B. (A) 426 Section parallel to the margin showing the erosional character of Channel B within a graben. 427 Black arrows mark strata truncation. Flow within the channel is northeastwards. (B) Distal 428 deep-sea lobe associated with Channel B. (C) Detail of the seafloor incision and associated 429 levees. Messinian Salt is pink, and sand-rich channels and lobe deposits are yellow. 430

431

- 432 ¹Supplemental Material. The uninterpreted version of the seismic data showed in the
- 433 manuscript. Please visit https://doi.org/10.1130/XXXX to access the supplemental material,
- and contact editing@geosociety.org with any questions.





Amplitude

1km

